

Interpretable Signed Link Prediction with Signed Infomax Hyperbolic Graph

Yadan Luo, Zi Huang, Hongxu Chen, Yang Yang and Mahsa Baktashmotlagh

Abstract—Signed link prediction in social networks aims to reveal the underlying relationships (*i.e.* links) among users (*i.e.* nodes) given their existing positive and negative interactions observed. Most of the prior efforts are devoted to learning node embeddings with graph neural networks (GNNs), which preserve the signed network topology by message-passing along edges to facilitate the downstream link prediction task. Nevertheless, the existing graph-based approaches could hardly provide human-intelligible explanations for the following three questions: (1) which neighbors to aggregate, (2) which path to propagate along, and (3) which social theory to follow in the learning process. To answer the aforementioned questions, in this paper, we investigate how to reconcile the *balance* and *status* social rules with information theory and develop a unified framework, termed as Signed Infomax Hyperbolic Graph (SIHG). By maximizing the mutual information between edge polarities and node embeddings, one can identify the most representative neighboring nodes that support the inference of edge sign. Different from existing GNNs that could only group features of friends in the subspace, the proposed SIHG incorporates the signed attention module, which is also capable of pushing hostile users far away from each other to preserve the geometry of antagonism. The polarity of the learned edge attention maps, in turn, provides interpretations of the social theories used in each aggregation. In order to model high-order user relations and complex hierarchies, the node embeddings are projected and measured in a hyperbolic space with a lower distortion. Extensive experiments on four signed network benchmarks demonstrate that the proposed SIHG framework significantly outperforms the state-of-the-arts in signed link prediction.

Index Terms—link prediction; signed social network; mutual information maximization; hyperbolic graph network.

1 INTRODUCTION

Understanding social interactions on the Web is critical for a broad set of tasks, such as community detection [1]–[3], personalized recommendation [4], [5], fake account detection [6] and event prediction [7]. By giving thumbs up, following and subscribing, users expose their positive preferences, support and approval for others who share the same opinions. Users also link to signify disapproval, disagreement, or distrust of others with negative response such as blocking. In such a signed social network, users or entities of interest are generally represented as nodes, and the mutual interactions are modeled as edges (or links) with signs.

While important, the interplay of positive and negative relations poses a great challenge to the vast majority of conventional online social network research that only considers observed connections as positive links, which refers to *unsigned* networks. Dedicated network embedding methods for unsigned networks [8]–[14] developed in the past, have exploited the fact that the node embeddings are highly correlated with the link structure of the network. These algorithms, therefore, predominantly focus on node representations and force the connected nodes to have similar latent features to preserve both local connectivity and

the high-order proximity among nodes in a graph. By using the low-dimensional node vectors, traditional machine learning methods can be applied to predict the connectivity between an arbitrary pair of nodes. However, for the real-life networks which consist of both positive and negative links (*i.e.* signed networks), the existing unsigned link prediction techniques are not directly applicable by virtue of lacking a specific mechanism to deal with the negative connections.

With a rapid development of graph neural networks (GNNs), recent works of SGCN [15] and SNEA [16] have been focusing on re-designing deep graph models to work with *signed* and undirected graph structures, where node features are recursively aggregated with adjacent nodes along signed edges. The core idea is based on one of the well-known social theories, the **structural balance theory** [17]. It roughly implies that attitudes of a user can change based on the assumption that a user's *friends of friends* can be deduced as friends, while *enemies of friends* can be considered as *enemies*. Nevertheless, as the balance rule is only tenable under certain circumstances, the **status theory** [18]–[20] is developed, which states that the signed links can be inferred by comparing the users' social status.

As modern social networks are complex and evolve quickly, user preferences or opinions remain uncertain and unstable. Before reaching the convergence, the underlying signed links cannot be explicitly predicted by either social theory. For instance, as shown in Figure 1, given the positive link from user k to user j and the negative link from user j to user i , user k will be predicted as an enemy of user i based on the **balance theory**, while as a friend if it is based on the **status theory**. Thereby, in our work, we aim to better comprehend the complex interplay between these two social theories and jointly accommodate them in one

- Y. Luo, Z. Huang and M. Baktashmotlagh are with School of Information Technology and Electrical Engineering, The University of Queensland, Brisbane 4072, Australia. E-mail: lyadanluo@gmail.com, huang@itee.uq.edu.au, m.baktashmotlagh@uq.edu.au.
- H. Chen is with the School of Computer Science in University of Technology Sydney, Sydney 2007, Australia. E-mail: hongxu.chen@uts.edu.au.
- Y. Yang is with the Center for Future Media and the School of Computer Science and Engineering, University of Electronic Science and Technology of China. E-mail: dlyyang@gmail.com.

Manuscript received November 25, 2020.

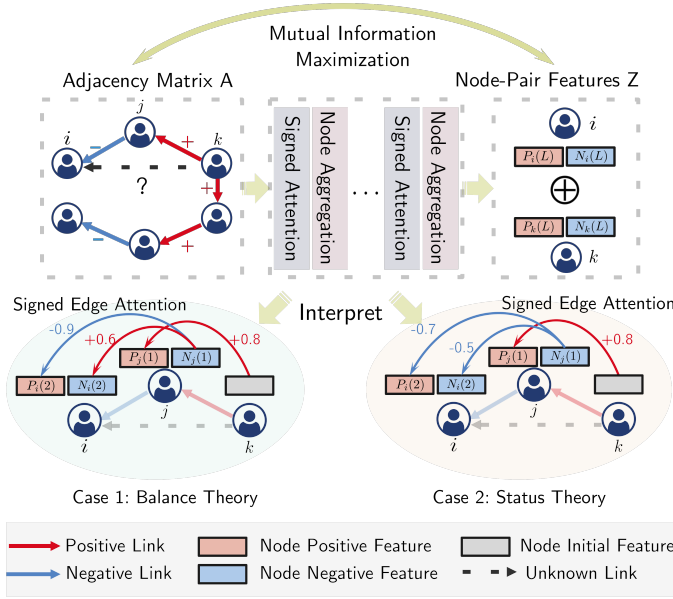


Fig. 1: An illustration of the interpretability of the proposed model for signed social networks. The learned signed attention maps are optimized by maximizing the mutual information between the node representations and the given edge polarity, which provide cues for discovering the underlying social theories.

unified framework to provide reasonable explanations of the user interactions at the current stage.

Even though one of recent work [21] that attempts to combine two social theories by manually defining 38 different types of local network motifs for guiding aggregation, it is still non-trivial to propose such a unified framework due to the following three challenges:

- The existing graph-based models generally lack interpretability in a sense that they do not easily allow for human-intelligible explanations of the following questions: for each target node-pair, (1) which neighboring nodes are decision-critical? (2) how to design the aggregation path for multi-hop neighbors? and (3) which social theory can be referred to? While the first two questions can be answered by inferring edge attention scores [16], [21], the last one has not yet been investigated.
- On the one hand, manually defining local motifs for aggregation is tedious and time-consuming especially in presence of massive number of adjacent neighbors. On the other hand, automatically embedding complex hierarchical neighborhood structures in GCNs or GAT can incur a large distortion [22], [23]. Such a dilemma forces common graph-based models to trade off between human-labors and prediction accuracy.
- Existing graph models do not define an inverse operation of grouping features, which means that features of negative pairs could hardly be pushed away from each other in the embedding space.

Core idea: To address the first challenge of endowing the models with interpretability, we demonstrate our core idea

in Figure 1. Inspired by recent advances in information theory, our strategy is to learn the optimal signed edge attention scores by maximizing the mutual information between the adjacency matrix of the observed social networks and the concatenated representations of the node pairs. By doing so, (1) the target nodes can automatically identify the most representative positive or negative neighbors multi-hops away that could support the prediction of the given edge polarity; (2) the explanations for each aggregation can be discovered by comparing the signs of the learned attention scores. For example, when aggregating the user j 's negative features $N_j(1)$ at the first graph layer to the user i 's negative features $N_i(2)$ at the second layer, one can identify the balance theory is applied if the attention score is positive; otherwise, the status rule is leveraged in this aggregation.

Specifically, in this paper, we propose a novel Signed Infomax Hyperbolic Graph (SIHG) network to reconcile *balance* and *status* theories in the task of signed link prediction. In order to fully inherit the rich hierarchical information in signed graphs, we generalize graph neural network to operate on a non-Euclidean space, where features from positive neighbors and negative neighbors are separately aggregated in different hyperbolic manifolds. To jointly realize the inclusion of features for friends and exclusion for foes in the embedding space, a signed attention mechanism is further incorporated, where positively linked nodes are mapped to close-by points whereas negatively linked nodes are transformed far from each other in hyperbolic manifolds. In line with the mutual information estimation, the learned attention scores provide interpretable explanations of social theories. As the proposed SIHG is agnostic to the choice of hyperbolic models, two hyperbolic models are testified in our framework. Extensive experiments conducted on four signed social network benchmarks evidence the superiority of the derived SIHG over the state-of-the-art approaches. In summary, our contribution is four-fold.

- We introduce a new Signed Infomax Hyperbolic Graph (SIHG) framework for signed link prediction, which unifies two social theories and provides human-intelligible interpretations by maximizing mutual information (addressing challenge 1).
- The projected hyperbolic space fully exploits the topology of users' positive and negative neighborhoods and learns the respective geometrical representations. Two hyperbolic models of Hyperboloid and Poincaré Ball are testified in our framework (addressing challenge 2).
- By incorporating the mutual information estimation, the derived signed attention module not only automatically learns the aggregation paths, but also pushes the hostile user nodes far away from each other (addressing challenge 3).
- We have demonstrated the effectiveness and interpretability of the proposed SIHG through extensive quantitative experiments and qualitative visualizations on four large-scale signed social network datasets. Source code¹ is provided for reference.

1. <https://anonymous.4open.science/r/cb105867-ad46-4bdd-97bf-092bf52d62d9/>

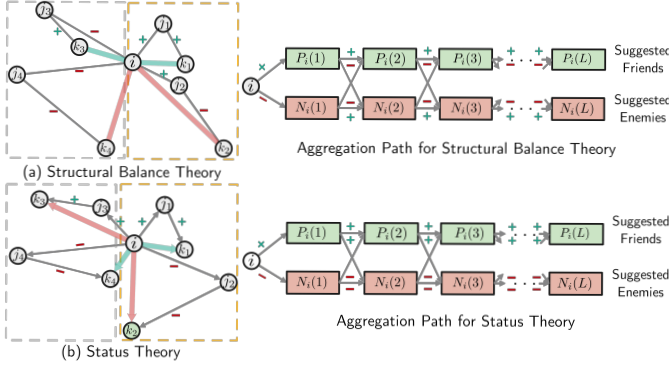


Fig. 2: An illustration of the (a) structural balance and (b) status theories, and the suggested aggregation paths.

The rest of paper is organized as follows. Section 2 introduces the mathematical definition of the signed link prediction task and theoretical foundations of signed social networks, followed by the details of the proposed SIHG model. The experimental comparisons with state-of-the-art, ablation study and visualizations are highlighted in Section 4. Section 5 presents a brief review of recent advances in signed link prediction and mutual information estimation. We conclude in Section 6.

2 PRELIMINARIES

2.1 Problem Definition

A signed social network can either be modeled as a directed or undirected graph $\mathcal{G} = (\mathcal{V}, \mathcal{E}^+, \mathcal{E}^-)$ with a sign on each edge $e_{ij} \in \mathcal{E}^+ \cup \mathcal{E}^-$, where the vertices $\mathcal{V} = \{v_i\}_{i=1}^N$ represent a set of N users. The initial feature for each node is denoted as $v_i \in \mathcal{V}$ with $x_i \in \mathbb{R}^d$, where d is the dimension of node embeddings. $\mathbf{A} \in \mathbb{R}^{N \times N}$ is the adjacency matrix of the signed network, where $A_{ij} = 1$, if there is a positive link from v_i to v_j , and $A_{ij} = 0$ for a negative link. For all A_{ij} which are equal to 0.5, there is no directed edge from v_i to v_j . Positive edges $\mathcal{E}^+ = \{e_{ij} | A_{ij} = 1\}_{i,j=1}^N$, and negative edges $\mathcal{E}^- = \{e_{ij} | A_{ij} = 0\}_{i,j=1}^N$ are partially observed at the training stage. The signed link prediction problem which we address here is to predict if a pair of nodes in \mathcal{V} will remain disconnected or will be connected by a positive or negative link.

2.2 Balance and Status Theories

We start by introducing the two fundamental social-psychological theories, which are illustrated in Figure 2. Structural balance theory [20] is based on the common principles that “the friend of my friend is my friend” and “the foe of my friend is my foe”. For instance, in Figure 2(a), if node v_{k_1} forms a triad with the edge e_{ij_1} , the triangle on (v_i, v_{j_1}, v_{k_1}) should have an odd number of positive signs regardless of edge direction. Those triads that obey structural balance theory refer to *balanced triangles*, such as (v_i, v_{j_1}, v_{k_1}) and (v_i, v_{j_2}, v_{k_2}) shown in the yellow dotted box. Otherwise, they are called as unbalanced triangles as highlighted in the grey dotted box. Alternatively, another theory is developed based on the notion of status [18], [19], as shown in Figure 2(b). The status theory posits that, in a

positive edge e_{ij} , user i regards user j as having a higher status, while in a negative edge e_{ij} , user i regards user j as having a lower status. By assuming that all nodes follow the status ordering, the edge sign should flip if its direction is flipped. Based on different social theories, the latent representation of each node i in a signed graph will be updated along various aggregation paths, which are demonstrated in Figure 2. For instance, according to balance theory, the first-order positive neighbors (e.g. v_{j_2}) of node v_i and the second-order negative neighbors (v_{k_2}) will be grouped in $P_i(1)$ and $N_i(2)$, respectively. To this end, the edge polarity between v_i and v_{k_2} can be inferred by measuring the similarity of the respective node embeddings.

Discussion. By comparing each of four typical types of signed triangles, the following two observations can be drawn:

- 1) The edge sign cannot be simply inferred by either of the theories, due to the conflicts in some cases. For example, the triangle (i, j_2, k_2) that satisfies status theory are not balanced.
- 2) For the same signed social network, the learned node embeddings can still vary significantly according to different theories. For example, with negative links e_{ij_2} and $e_{j_2k_2}$, the representation of node v_{k_2} should be far from the feature of node v_i in status theory, which is opposite to the situation in balance theory.

Motivated by the observations mentioned above, we aim to derive a unified framework that dynamically chooses a proper path to aggregate node embeddings and predict edge polarities. The core principle behind the framework is to infer the missing signs of edges that provides interpretable explanations for the given edge labels, which can be achieved by maximizing the mutual information in the signed social networks.

3 METHODOLOGY

In this section, we go through the details of the proposed Signed Infomax Hyperbolic Graph (SIHG) framework as illustrated in Figure 3. In order to propagate positive and negative neighbors’ information hierarchically and structurally, we construct two L -layer hyperbolic graph sub-networks, i.e., $\mathcal{G}_P = \{\mathcal{G}_P^{(l),H} = (\mathcal{V}^{P(l),H}, \mathcal{E}^+, \mathcal{E}^-)\}_{l=1}^L$ and $\mathcal{G}_N = \{\mathcal{G}_N^{(l),H} = (\mathcal{V}^{N(l),H}, \mathcal{E}^+, \mathcal{E}^-)\}_{l=1}^L$ for passing messages L -hops away. The superscript H denotes hyperbolic embedding and the superscripts P and N indicate the positive and negative semantics, respectively. Each positive node $v_i^{P(l),H} \in \mathcal{V}^{P(l),H}$ and each negative node $v_i^{N(l),H} \in \mathcal{V}^{N(l),H}$ at the l -th layer are associated with hidden features of $h_i^{P(l),H} \in \mathbb{H}^{d,K}$ and $h_i^{N(l),H} \in \mathbb{H}^{d,K}$, where $\mathbb{H}^{d,K}$ is the hyperbolic manifold in d dimensions with constant negative curvature $c = -1/K$ ($K > 0$). As the input node feature $x_i^{0,E} \in \mathbb{R}^d$ is in a Euclidean space (denoted with the superscript E), we first transform it to the hyperbolic space via the \exp_o map (Section 3.1), and then leverage the signed attention strategy to aggregate the features from neighborhoods (Section 3.2). The aggregation is guided by maximizing the mutual information between

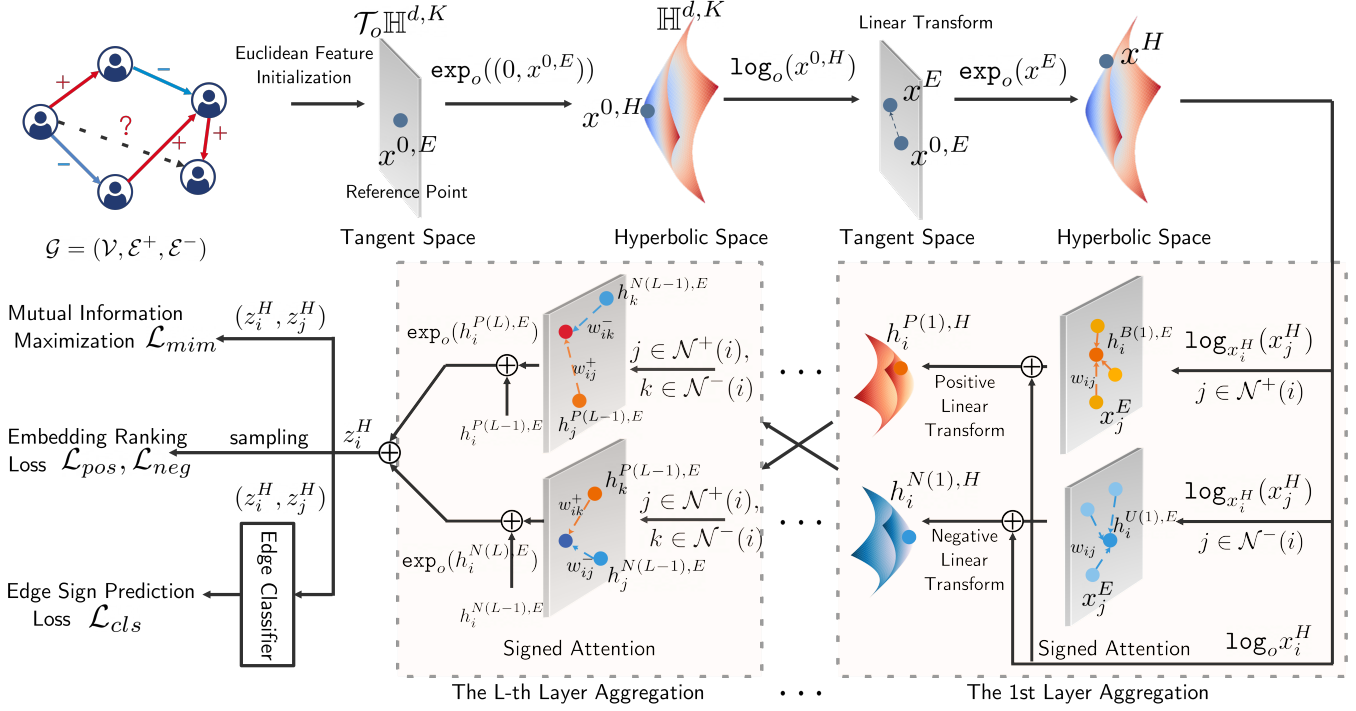


Fig. 3: An overview of the proposed Signed Infomax Hyperbolic Graph (SIHG) architecture with L graph layers.

the concatenated node features and edge signs, as discussed in Section 3.3. To this end, two fundamental social theories can be seamlessly reconciled and interpreted by the learned attention maps.

3.1 Hyperbolic Transformation

Before formalizing the hyperbolic transformations for input Euclidean node features, we start by outlining a relationship between the Euclidean space and Hyperbolic space. A hyperbolic space is a homogeneous space that has a constant negative curvature, which is distinguished from Euclidean spaces with zero curvature ($c = 0$). While the tangent spaces of the points on hyperbolic manifold are isometric to \mathbb{R}^d , the Euclidean transformation can be performed in $\mathcal{T}_o \mathbb{H}^{d,K}$, where $o := \{\sqrt{K}, 0, \dots, 0\} \in \mathbb{H}^{d,K}$ is the origin in $\mathbb{H}^{d,K}$. Motivated by this, we regard $(0, x^{0,E})$ as a point in the tangent space $\mathcal{T}_o \mathbb{H}^{d,K}$ and project it to hyperbolic space by \exp_o map, where o serves as a reference point to :

$$\mathbf{x}^{0,H} = \exp_o(0, \mathbf{x}^{0,E}), \quad (1)$$

with $\mathbf{x}^{0,H}$ the corresponding point in $\mathbb{H}^{d,K}$. For linear transformation of a point in a Hyperbolic space, we define the following operations:

$$\begin{aligned} \mathbf{x}^H &= \mathbf{W} \otimes^H \mathbf{x}^{0,H} \oplus^H \mathbf{b}, \\ \mathbf{W} \otimes^H \mathbf{x} &:= \phi \exp_o(\mathbf{W} \log_o(\mathbf{x})), \\ \mathbf{x} \oplus^H \mathbf{b} &:= \exp_x(P_{o \rightarrow x}^K(\mathbf{b})), \end{aligned} \quad (2)$$

where $\mathbf{W} \in \mathbb{R}^{d \times d}$ is a learnable weight matrix, and $\mathbf{b} \in \mathbb{R}^d$ is a bias. The $P_{o \rightarrow x}^K(\cdot)$ is the parallel transport from $\mathcal{T}_o \mathbb{H}^{d,K}$ to $\mathcal{T}_x \mathbb{H}^{d,K}$. There are several important models of hyperbolic space such as the Klein model, Hyperboloid model, and Poincaré ball model, in which the differentiable operations

\log and \exp can be implemented differently. Any two of the aforementioned models can be related by a transformation that preserves all the geometrical properties of the space, including isometry. Without loss of generality, here, we introduce the following two hyperbolic models in our framework:

3.1.1 Hyperboloid Model

The hyperboloid model, also called as Lorentz model, is defined as $\mathbb{H}^{d,K} := \{\mathbf{x} \in \mathbb{R}^{d+1} : \langle \mathbf{x}, \mathbf{x} \rangle_L = -K, x_0 > 0\}$, where $\langle \cdot, \cdot \rangle_L : \mathbb{R}^{d+1} \times \mathbb{R}^{d+1} \rightarrow \mathbb{R}$ indicating the Minkowski inner product, specifically $\langle \mathbf{x}, \mathbf{y} \rangle_L := -x_0 y_0 + x_1 y_1 + \dots + x_d y_d$. The tangent space centered at point \mathbf{x} is $\mathcal{T}_x \mathbb{H}^{d,K} := \{\mathbf{v} \in \mathbb{R}^{d+1} : \langle \mathbf{v}, \mathbf{x} \rangle_L = 0\}$. The mapping between tangent space and hyperbolic space is through exponential and logarithmic maps, respectively. The exponential map $\exp_x : \mathcal{T}_x \mathbb{H}^{d,K} \rightarrow \mathbb{H}^{d,K}$, and the logarithmic map $\log_x : \mathbb{H}^{d,K} \rightarrow \mathcal{T}_x \mathbb{H}^{d,K}$ of the hyperboloid model are given by:

$$\begin{aligned} \exp_x(\mathbf{v}) &= \cosh\left(\frac{\|\mathbf{v}\|_L}{\sqrt{K}}\right) \mathbf{x} + \sqrt{K} \sinh\left(\frac{\|\mathbf{v}\|_L}{\sqrt{K}}\right) \frac{\mathbf{v}}{\|\mathbf{v}\|_L}, \\ \log_x(\mathbf{y}) &= \text{Dist}(\mathbf{x}, \mathbf{y}) \frac{\mathbf{y} + \frac{1}{K} \langle \mathbf{x}, \mathbf{y} \rangle_L \mathbf{x}}{\|\mathbf{y} + \frac{1}{K} \langle \mathbf{x}, \mathbf{y} \rangle_L \mathbf{x}\|_L}, \\ \text{Dist}(\mathbf{x}, \mathbf{y}) &= \sqrt{K} \text{arcosh}(-\langle \mathbf{x}, \mathbf{y} \rangle_L / K), \end{aligned} \quad (3)$$

where $\mathbf{v} \in \mathcal{T}_x \mathbb{H}^{d,K}$ and $\mathbf{x}, \mathbf{y} \in \mathbb{H}^{d,K}$. $\text{Dist}(\mathbf{x}, \mathbf{y})$ indicate the intrinsic distance between two points \mathbf{x} and \mathbf{y} in $\mathbb{H}^{d,K}$. We denote $\|\mathbf{v}\|_L = \sqrt{\langle \mathbf{v}, \mathbf{v} \rangle_L}$ as the norm of $\mathbf{v} \in \mathcal{T}_x \mathbb{H}^{d,K}$.

3.1.2 Poincaré Ball Model

The Poincaré Ball model with constant negative curvature ($c = -\frac{1}{K}, K > 0$) is an open unit ball, i.e., $\mathbb{H}^{d,K} := \{\mathbf{x} \in$

$\mathbb{R}^d : \|\mathbf{x}\| < 1$. For any point $\mathbf{x} \in \mathbb{H}^{d,K}$, the exponential map $\exp_{\mathbf{x}} : \mathcal{T}_{\mathbf{x}}\mathbb{H}^{d,K} \rightarrow \mathbb{H}^{d,K}$ and the logarithmic map $\log_{\mathbf{x}} : \mathbb{H}^{d,K} \rightarrow \mathcal{T}_{\mathbf{x}}\mathbb{H}^{d,K}$ are defined, respectively, as:

$$\exp_{\mathbf{x}}(\mathbf{v}) = \mathbf{x} \oplus \left(\tanh\left(\frac{\|\mathbf{v}\|}{\sqrt{K}(1 - \frac{1}{K}\|\mathbf{x}\|^2)}\right) \frac{\mathbf{v}}{\sqrt{K}\|\mathbf{v}\|} \right),$$

$$\log_{\mathbf{x}}(\mathbf{y}) = \sqrt{K}(1 - \frac{1}{K}\|\mathbf{x}\|^2) \operatorname{arctanh}\left(\frac{1}{\sqrt{K}}\|\mathbf{y} - \mathbf{x} \oplus \mathbf{y}\|\right) \frac{-\mathbf{x} \oplus \mathbf{y}}{\|\mathbf{y} - \mathbf{x} \oplus \mathbf{y}\|} \quad (4)$$

$$\operatorname{Dist}(\mathbf{x}, \mathbf{y}) = 2\sqrt{K} \operatorname{arctanh}\left(\frac{1}{\sqrt{K}}\|\mathbf{y} - \mathbf{x} \oplus \mathbf{y}\|\right),$$

where \oplus is the Mobius addition for any $\mathbf{x}, \mathbf{y} \in \mathbb{H}^{d,K}$. Mobius addition is defined as,

$$\mathbf{x} \oplus \mathbf{y} = \frac{(1 + \frac{2}{K}\langle \mathbf{x}, \mathbf{y} \rangle + \frac{1}{K}\|\mathbf{y}\|^2)\mathbf{x} + (1 - \frac{1}{K}\|\mathbf{x}\|^2)\mathbf{y}}{1 + \frac{2}{K}\langle \mathbf{x}, \mathbf{y} \rangle + \frac{1}{K^2}\|\mathbf{x}\|^2\|\mathbf{y}\|^2}, \quad (5)$$

with $\langle \cdot, \cdot \rangle$ being the inner product.

3.2 Signed Neighbor Aggregation

In this section, we discuss how to aggregate node's information from its positive and negative neighborhood after obtaining the transformed features on the hyperbolic space. We first define the set of positive and negative neighbors of a user i to be $\mathcal{N}^+(i)$ and $\mathcal{N}^-(i)$, respectively. For the first aggregation layer, we have

$$\mathbf{h}_i^{P(1),H} = \exp_{\mathbf{x}_i^H} \left(\sigma(\mathbf{W}_p^{(1)} [\sum_{j \in \mathcal{N}^+(i)} \mathbf{w}_{ij}^{+(1)} \log_{\mathbf{o}}(\mathbf{x}_j^H), \mathbf{x}_i^H]) \right),$$

$$\mathbf{h}_i^{N(1),H} = \exp_{\mathbf{x}_i^H} \left(\sigma(\mathbf{W}_n^{(1)} [\sum_{j \in \mathcal{N}^-(i)} \mathbf{w}_{ij}^{-(1)} \log_{\mathbf{o}}(\mathbf{x}_j^H), \mathbf{x}_i^H]) \right),$$

$$\mathbf{w}_{ij}^{+(1)} = \mathcal{F}_{j \in \mathcal{N}^+(i)} \left(\sigma(\mathbf{a}_p^{(1)T} [\mathbf{W}_{pw}^{(1)} \log_{\mathbf{o}} \mathbf{x}_i^H, \mathbf{W}_{pw}^{(1)} \log_{\mathbf{o}} \mathbf{x}_j^H]) \right),$$

$$\mathbf{w}_{ij}^{-(1)} = \mathcal{F}_{j \in \mathcal{N}^-(i)} \left(\sigma(\mathbf{a}_n^{(1)T} [\mathbf{W}_{nw}^{(1)} \log_{\mathbf{o}} \mathbf{x}_i^H, \mathbf{W}_{nw}^{(1)} \log_{\mathbf{o}} \mathbf{x}_j^H]) \right), \quad (6)$$

where the function $\mathcal{F}_{j \in \mathcal{N}^{\pm}(i)}(\mathbf{x}) = (2e^{\mathbf{x}_i} / \sum_j e^{\mathbf{x}_j}) - 1$ regularizes the attention weights $w_{ij}^{+(1)}, w_{ij}^{-(1)}$ in a range of $(-1, 1)$. $\mathbf{W}_p^{(1)}, \mathbf{W}_n^{(1)} \in \mathbb{R}^{d \times 2d}$, $\mathbf{a}_p^{(1)}, \mathbf{a}_n^{(1)} \in \mathbb{R}^{2d \times d}$, and $\mathbf{W}_{pw}^{(1)}, \mathbf{W}_{nw}^{(1)} \in \mathbb{R}^{d \times d}$ are the weight matrices. $\sigma(\cdot)$ is the LeakyReLU activation, with $[\cdot, \cdot]$ being the concatenation operation. The hidden representation $\mathbf{h}_i^{P(1),H} \in \mathbb{H}^{d,K}$ and $\mathbf{h}_i^{N(1),H} \in \mathbb{H}^{d,K}$ collect the positive and negative supports from the adjacent positive neighbors, respectively, which allow to embed node features close to positive neighbors and distant to negative neighbors. However, for multi-hop neighborhood, the relationships become complex to determine. According to Figure 2, the aggregation rule for $l > 1$

is defined as,

$$\hat{\mathbf{h}}_i^{P(l),H} = \left[\sum_{j \in \mathcal{N}^+(i)} \mathbf{w}_{ij}^{+(l)} \log_{\mathbf{o}}(\mathbf{h}_j^{P(l-1),H}), \sum_{k \in \mathcal{N}^-(i)} \mathbf{w}_{ik}^{-(l)} \log_{\mathbf{o}}(\mathbf{h}_k^{N(l-1),H}) \right],$$

$$\hat{\mathbf{h}}_i^{N(l),H} = \left[\sum_{j \in \mathcal{N}^-(i)} \mathbf{w}_{ij}^{-(l)} \log_{\mathbf{o}}(\mathbf{h}_j^{N(l-1),H}), \sum_{k \in \mathcal{N}^+(i)} \mathbf{w}_{ik}^{+(l)} \log_{\mathbf{o}}(\mathbf{h}_k^{P(l-1),H}) \right],$$

$$\mathbf{h}_i^{P(l),H} = \exp_{\mathbf{h}_i^{P(l-1),H}} \left(\sigma(\mathbf{W}_p^{(l)} [\hat{\mathbf{h}}_i^{P(l),H}, \mathbf{h}_i^{P(l-1),H}]) \right),$$

$$\mathbf{h}_i^{N(l),H} = \exp_{\mathbf{h}_i^{N(l-1),H}} \left(\sigma(\mathbf{W}_n^{(l)} [\hat{\mathbf{h}}_i^{N(l),H}, \mathbf{h}_i^{N(l-1),H}]) \right), \quad (7)$$

$$\mathbf{w}_{ij}^{+(l)} = \mathcal{F}_{j \in \mathcal{N}^+(i)} \left(\sigma(\mathbf{a}_p^{(l)T} [\mathbf{W}_{pw}^{(l)} \log_{\mathbf{o}} \mathbf{h}_i^{P(l-1),H}, \mathbf{W}_{pw}^{(l)} \log_{\mathbf{o}} \mathbf{h}_j^{P(l-1),H}]) \right),$$

$$\mathbf{w}_{ij}^{-(l)} = \mathcal{F}_{j \in \mathcal{N}^-(i)} \left(\sigma(\mathbf{a}_n^{(l)T} [\mathbf{W}_{nw}^{(l)} \log_{\mathbf{o}} \mathbf{h}_i^{N(l-1),H}, \mathbf{W}_{nw}^{(l)} \log_{\mathbf{o}} \mathbf{h}_j^{N(l-1),H}]) \right),$$

$$\mathbf{w}_{ik}^{+(l)} = \mathcal{F}_{k \in \mathcal{N}^+(i)} \left(\sigma(\mathbf{a}_p^{(l)T} [\mathbf{W}_{pw}^{(l)} \log_{\mathbf{o}} \mathbf{h}_i^{N(l-1),H}, \mathbf{W}_{pw}^{(l)} \log_{\mathbf{o}} \mathbf{h}_k^{P(l-1),H}]) \right),$$

$$\mathbf{w}_{ik}^{-(l)} = \mathcal{F}_{k \in \mathcal{N}^-(i)} \left(\sigma(\mathbf{a}_n^{(l)T} [\mathbf{W}_{pw}^{(l)} \log_{\mathbf{o}} \mathbf{h}_i^{P(l-1),H}, \mathbf{W}_{nw}^{(l)} \log_{\mathbf{o}} \mathbf{h}_k^{N(l-1),H}]) \right),$$

with $\mathcal{F}_{j \in \mathcal{N}^{\pm}(i)}(\mathbf{x}) = (2e^{\mathbf{x}_i} / \sum_j e^{\mathbf{x}_j}) - 1$. Similarly, $\mathbf{W}_p^{(l)}, \mathbf{W}_n^{(l)} \in \mathbb{R}^{d \times 2d}$, $\mathbf{a}_p^{(l)}, \mathbf{a}_n^{(l)} \in \mathbb{R}^{2d \times d}$ and $\mathbf{W}_{pw}^{(l)}, \mathbf{W}_{nw}^{(l)} \in \mathbb{R}^{d \times d}$ are learnable weight matrices. The final representation $\mathbf{z}_i^H \in \mathbb{H}^{d,K}$ for each node i at the L -th layer can be obtained by,

$$\mathbf{z}_i^H = [\mathbf{h}_i^{P(L),H}, \mathbf{h}_i^{N(L),H}]. \quad (8)$$

3.3 Mutual Information Maximization

For guiding the path of aggregation between balance theory and status theory, a Shannon entropy-based measure, *i.e.*, Mutual information (MI) is leveraged to measure the correlations between the adjacency matrix \mathbf{A} and the concatenated representations of node-pairs \mathbf{Z} , with $\mathbf{z}_{ij} = [\mathbf{z}_i^H, \mathbf{z}_j^H] \in \mathbb{H}^{2d,K}$. Based on the principle of [24], [25], the mutual information $I(\mathbf{Z}, \mathbf{A})$ is equivalent to the Kullback-Leibler (KL) divergence between the joint and product of the marginals, $\mathbb{J} = \mathbb{P}_{\mathbf{Z}\mathbf{A}}$ and $\mathbb{M} = \mathbb{P}_{\mathbf{Z}} \otimes \mathbb{P}_{\mathbf{A}}$:

$$I(\mathbf{Z}, \mathbf{A}) = D_{KL}(\mathbb{J} \parallel \mathbb{M}). \quad (9)$$

The larger the divergence between the joint and the product of the marginals, the stronger the dependence between \mathbf{Z} and \mathbf{A} . Maximizing mutual information forces the node embeddings to aggregate features from their positive and negative neighbors within L hops. According to the Donsker-Varadhan representation [26] of the KL-divergence, the lower-bound to the mutual information can be derived as,

$$D_{KL}(\mathbb{J} \parallel \mathbb{M}) \geq \hat{I}_{\theta}(\mathbf{Z}, \mathbf{A}) := \sup_{\theta \in \Theta} \mathbb{E}_{\mathbb{J}}[T_{\theta}(\mathbf{Z}, \mathbf{A})] - \log \mathbb{E}_{\mathbb{M}}[e^{T_{\theta}(\mathbf{Z}, \mathbf{A})}], \quad (10)$$

where $T_{\theta} : \mathbf{Z} \times \mathbf{A} \rightarrow \mathbb{R}$ is a discriminator function modeled by a neural network parameterized by θ . The expectations in Equation (10) are estimated using i.i.d samples from the joint distribution \mathbb{J} and shuffled samples from the respective marginal distributions. The objective function in Equation (11) can be maximized by gradient ascent, as:

$$\mathcal{L}_{mim} = -\hat{I}_{\theta}(\mathbf{Z}, \mathbf{A}). \quad (11)$$

3.4 Edge Classifier and Training Objectives

For the task of signed link prediction, we use the Fermi-Dirac decoder to generate the predictions, which are supervised by a binary cross entropy loss:

$$p_{ij} = [e^{(\operatorname{Dist}(\mathbf{z}_i^H, \mathbf{z}_j^H)^2 - r)/t}]^{-1},$$

$$\mathcal{L}_{cls} = \sum_{i,j \in \mathcal{V}} \mathbf{A}_{ij} \log(p_{ij}) + (1 - \mathbf{A}_{ij}) \log(1 - p_{ij}), \quad (12)$$

with r and t being the hyperparameters. To further constrain the node embeddings, we design a positive ranking loss and a negative ranking loss, respectively. For each positive or negative pair of users (i, j) , we randomly sample a neutral user k which has no link to the anchor i . The following objectives enable the positively linked users closer (and negatively linked users farther) in the embedded space than the no-link pairs (i, k) :

$$\begin{aligned}\mathcal{L}_{pos} &= \sum_{(i,j) \in \mathcal{E}^+, k} \max(0, \text{Dist}(z_i^H, z_j^H) - \text{Dist}(z_i^H, z_k^H)), \\ \mathcal{L}_{neg} &= \sum_{(i,j) \in \mathcal{E}^-, k} \max(0, \text{Dist}(z_i^H, z_k^H) - \text{Dist}(z_i^H, z_j^H)).\end{aligned}\quad (13)$$

Lastly, the model is jointly trained by edge classification loss, mutual information loss, and two embedding losses:

$$\mathcal{L} = \mathcal{L}_{cls} + \alpha \mathcal{L}_{pos} + \beta \mathcal{L}_{neg} + \gamma \mathcal{L}_{mim}, \quad (14)$$

where α , β , and γ denote the loss coefficients, respectively.

4 EXPERIMENTAL SETTINGS

4.1 Datasets and Evaluation Metrics

In this section, we conduct extensive experiments on four real-world signed social network datasets, *i.e.*, Bitcoin-Alpha², Bitcoin-OTC³, Slashdot⁴, Epinions⁵. The general statistics of the four network datasets are summarized in Table 1.

- **Bitcoin-Alpha** and **Bitcoin-OTC** [27], [28] are two who-trusts-whom networks of Bitcoin trading. Members of Bitcoin Alpha and OTC rate other members as trust or distrust to prevent transactions from risky users.
- **Slashdot** [19] is collected from a technology-related news website known for its specific user community. The website features user-submitted and editor-evaluated technology oriented news. It allows users to tag each other as friends (positive links) or foes (negative links).
- **Epinions** [19] is a trust network for the consumer review site. All the trust relationships interact and form the Web of Trust, which is then combined with review ratings to determine which reviews are shown to the user.

In order to predict the link relationship of the unconnected node pairs, we randomly select 20% of the links in the social networks to form a test set, with the remaining links as the training set. We utilize the standard metrics *i.e.*, area under curve (AUC), F1 score, **macro-averaged F1** score, and **micro-averaged F1** score to evaluate the prediction performance.

2. <http://www.btcalpha.com/>

3. <http://www.bitcoin-otc.com/>

4. <http://slashdot.org/>

5. <http://www.epinions.com/>

4.2 Baselines Methods

We compare our approach with the following signed network embedding and link prediction methods:

- **TSVD** [29]: performs linear dimensionality reduction by means of truncated singular value decomposition (SVD).
- **SSE** [30]: reformulates the Rayleigh quotient as an objective for embedding learning.
- **SiNE** [31]: optimizes an objective function guided by social theory in signed networks to generate the node embeddings in a deep learning framework.
- **SIDE** [32]: provides a linearly scalable method to obtain the low-dimensional vectors with random walks.
- **SIGNet** [33]: builds upon word2vec embedding approaches and adds a sampling strategy to maintain balance in high-order neighborhoods.
- **SGCN** [15]: generalizes GNNs to a signed network for the first time. It designs a new aggregation strategy for undirected signed network.
- **SiGAT** [21]: incorporates graph motifs into GAT to capture the balance theory and status theory jointly.
- **SNEA** [16]: proposes a graph attention layer to estimate the importance coefficients for the node pairs.

4.3 Implementation Details

Our source code is based on PyTorch [34], which is available in an anonymous repository⁶ for reference. All experiments are conducted on two servers with two GeForce GTX 2080 Ti GPUs. Similar to previous works in this area [15], random seed is set to 42. For fair comparisons, the feature dimensions of node embedding d are fixed to 64. The total number of training epochs M is 800 for Bitcoin-Alpha and Bitcoin-OTC datasets, 900 for Slashdot and Epinions datasets. The Adam optimizer is applied with a weight decay of 1×10^{-5} . The learning rate μ is initiated to be 1×10^{-2} for Bitcoin-Alpha and Bitcoin-OTC datasets, and 5×10^{-3} for Slashdot and Epinions datasets. The learning rate is adapted by a cosine annealing schedule. The node embedding is initialized with TruncatedSVD [29], with maximum 30 iterations. The optimal loss coefficients α , γ are searched with optuna [35] framework, and β is empirically set to 0.83 for all tasks. The hyperparameter r and t for edge classifier are fixed to 2 and 1, respectively. Without loss of generality, we set the curvature $K = 1$ (*i.e.* $c = -1$), which can be further tuned for \mathcal{G}_p and \mathcal{G}_n . The T_θ network firstly maps each node-pair representation / edge sign from 128-D / 1-D to 128-D with two fully connected layers. It then projects the addition of the two 128-D vectors to 1-D scores with a LeakyReLU and a fully connected layer.

5 EXPERIMENTAL RESULTS AND ANALYSIS

Following the settings in Section 4, we conduct experiments to evaluate the performance of the proposed SIHG regarding both the signed link prediction effectiveness and interpretation quality. In particular, we aim to answer the

6. <https://anonymous.4open.science/r/cb105867-ad46-4bdd-97bf-092bf52d62d9/>

TABLE 1: The general statistics of the four datasets used in our experiments.

Datasets	# Nodes	# Links	% Positive Links	% Negative Links
Bitcoin-Alpha	3,783	14,145	89.99	10.01
Bitcoin-OTC	5,881	21,522	85.45	14.55
Slashdot	82,140	549,202	77.40	22.60
Epinions	131,827	841,372	85.30	14.70

TABLE 2: AUC and F1 scores of predicting signed edges among four datasets.

Method	Bitcoin-Alpha		Bitcoin-OTC		Slashdot		Epinions	
	AUC	F1	AUC	F1	AUC	F1	AUC	F1
TSVD [29]	0.740	0.863	0.761	0.870	0.740	0.804	0.766	0.843
SSE [30]	0.764	0.898	0.803	0.923	0.769	0.820	0.822	0.901
SiNE [31]	0.781	0.895	0.782	0.876	0.785	0.850	0.831	0.902
SIDE [32]	0.642	0.753	0.632	0.728	0.554	0.624	0.617	0.725
SGCN [15]	0.801	0.915	0.804	0.908	0.786	0.859	0.849	0.920
SiGAT [21]	0.775	0.894	0.796	0.903	0.789	0.857	0.853	0.917
SNEA [16]	0.816	0.927	0.818	0.924	0.799	0.868	0.861	0.933
SIHG	0.898	0.961	0.915	0.953	0.895	0.919	0.926	0.957

following research questions (RQs) via experiments:

RQ1: How effectively can SIHG perform signed link prediction compared with state-of-the-art baselines?

RQ2: What is the contribution of each key component of the proposed model structure?

RQ3: How the hyperparameters affect the performance of SIHG in terms of prediction effectiveness?

RQ4: How is the quality of the learned node representations?

RQ5: How to interpret the underlying social theories with the learned signed attention maps?

5.1 Signed Link Prediction Effectiveness (RQ1)

In Table 2, we report the signed link prediction results across the four benchmark datasets in terms of **AUC** and **F1** scores. The baseline results refer to [15], [16]. The graph depth L is fixed to 3 and the Hyperboloid model is incorporated in **SIHG**. In order to fully investigate the graph-based baselines that are highly related to our work, we re-implement **SGCN**, **SiGAT**, and **SNEA**, and additionally report the **macro-F1** and **micro-F1** scores in Table 3. It is

TABLE 3: The signed link prediction results of the proposed method and compared baselines. * indicates the results of re-implementation.

Dataset	Method	AUC	F1	macro-F1	micro-F1
Bitcoin-Alpha	SGCN* [15]	0.8147	0.8996	0.6836	0.8310
	SiGAT* [21]	0.8393	0.9519	0.6721	0.9109
	SNEA* [16]	0.8293	0.9297	0.7430	0.8786
	SIHG	0.8981	0.9614	0.7115	0.9279
Bitcoin-OTC	SGCN* [15]	0.8087	0.9152	0.7617	0.8605
	SiGAT* [21]	0.8797	0.9423	0.7578	0.8983
	SNEA* [16]	0.8131	0.9174	0.7705	0.8646
	SIHG	0.9154	0.9528	0.7949	0.9165
Slashdot	SGCN* [15]	0.7827	0.8688	0.7512	0.8068
	SNEA* [16]	0.7918	0.8627	0.7634	0.8051
	SIHG	0.8950	0.9189	0.7934	0.8696
Epinions	SGCN* [15]	0.8331	0.8688	0.7512	0.8068
	SNEA* [16]	0.8542	0.9304	0.8167	0.8873
	SIHG	0.9262	0.9571	0.8261	0.9247

TABLE 4: Ablation study of the proposed SIHG on Bitcoin-Alpha and Bitcoin-OTC datasets.

			Bitcoin-Alpha		Bitcoin-OTC	
MIM	Signed Attention	Hyperbolic	AUC	F1	AUC	F1
-	-	-	0.8149	0.9020	0.8268	0.9297
✓	-	-	0.8867	0.9602	0.9071	0.9493
-	✓	-	0.8532	0.9571	0.8925	0.9456
-	-	✓	0.8756	0.9580	0.9004	0.9517
-	✓	✓	0.8767	0.9588	0.9034	0.9510
✓	✓	-	0.8880	0.9597	0.9115	0.9507
✓	-	✓	0.8817	0.9575	0.9133	0.9527
✓	✓	✓	0.8981	0.9614	0.9154	0.9528

TABLE 5: The link prediction performances of the proposed SIHG w.r.t. various hyperbolic models on 3 datasets.

Dataset	Method	AUC	F1	macro-F1	micro-F1
Bitcoin-Alpha	Euclidean	0.8880	0.9597	0.6934	0.9247
	Poincaré	0.8860	0.9600	0.6894	0.9251
	Hyperboloid	0.8981	0.9614	0.7115	0.9279
Bitcoin-OTC	Euclidean	0.9115	0.9507	0.7822	0.9125
	Poincaré	0.9071	0.9510	0.7826	0.9130
	Hyperboloid	0.9154	0.9528	0.7949	0.9165

observed that the proposed SIHG framework is superior to all the compared methods in most cases. Among the four commonly-used evaluation metrics, the AUC scores of SIHG are boosted by the largest margin (13.03% on Slashdot) over the best performing baseline, especially on the large-scale datasets, while the macro-F1 scores are slightly weaker. We infer this result is due to using macro-average, which computes the score independently for each class (*i.e.* $-1, 1$) and treats all classes equally. Therefore, using macro-F1 cannot fairly testify the prediction quality on extremely biased datasets such as signed social networks.

5.2 Ablation Study (RQ2)

To investigate the validity of the derived MI objective (**MIM**), the signed attention mechanism (**Signed Attention**) and the incorporated Hyperboloid models (**Hyperbolic**), we compare the seven variants of SIHG model on both **Bitcoin-Alpha** and **Bitcoin-OTC** datasets, and summarize the comparison results in Table 4. The graph depth L is fixed to 3 and loss coefficients α and γ are empirically fixed. The first row corresponds to the simplest baseline, which resembles SGCN yet it has separate transformations for positive and negative neighbors' features. By comparing the rest of variants with one or two components removed, we observed degradation in the respective performances of signed link prediction. It is noteworthy that removing the MI objective will lead to a significant drop in prediction accuracy, which verifies the importance of discovering correlations between the edge polarity and the latent node embedding pairs.

5.3 Parameter Sensitivity (RQ3)

We evaluate the sensitivity of the proposed SIHG method *w.r.t.* the choices of hyperbolic models, loss coefficients α and γ , and the depth L of graph networks on the Bitcoin-Alpha and Bitcoin-OTC datasets.

Effect of Hyperbolic Model. First, we assess the impact of the base model of the SIHG, *i.e.*, **Euclidean**, **Poincaré**, and **Hyperboloid** models *w.r.t.* four evaluation metrics. Notably,

TABLE 6: Prediction performance of the signed edges with respect to various graph depth on the two datasets.

Dataset	Method	AUC	F1	macro-F1	micro-F1
Bitcoin-Alpha	SIHG-1	0.8897	0.9597	0.6712	0.9244
	SIHG-2	0.8862	0.9612	0.7079	0.9276
	SIHG-3	0.8981	0.9614	0.7115	0.9279
	SIHG-4	0.8664	0.9602	0.8978	0.9255
Bitcoin-OTC	SIHG-1	0.9113	0.9505	0.7779	0.9121
	SIHG-2	0.9120	0.9505	0.7834	0.9123
	SIHG-3	0.9154	0.9528	0.7949	0.9165
	SIHG-4	0.9025	0.9515	0.7891	0.9142

for Euclidean model, we do not apply the \log and \exp maps. The results, reported in Table 5, demonstrate that the proposed SIHG framework with the hyperboloid model achieve a relatively higher performance compared to the Euclidean alternative, improving AUC scores from 88.8% to 89.8%. The performance improvement also illustrates the numerical stability of the Hyperboloid over the Poincaré.

Effect of Loss Coefficients. To study the effect of the loss coefficients, we conduct the experiments on the proposed SIHG with the varying values of α and γ . The remaining coefficient β is empirically set to 0.83. The search of the optimal loss coefficients is implemented with the optuna [35] toolbox. The Figure 5 is plotted based on the results from 100 trails, with α and γ ranging from 0 to 3. It can be observed that the AUC and F1 scores are going uphill when γ increases, which validates the importance of the derived mutual information maximization strategy. Another finding is that, the AUC and F1 scores become quite stable when reaching sufficiently large loss coefficients. This indicates that our SIHG framework is robust with respect to loss coefficients.

Effect of Graph Depth. To investigate the impact of the number of stacked graph layers, we examine the proposed SIHG framework with varying depth of graph layers, *i.e.*, $L \in \{1, 2, 3, 4\}$. As shown in Table 6, the performance of the proposed SIHG with deeper graph networks generally increases until L reaches 3. Due to the sparsity of signed networks and the intrinsic over-smoothing risk of GNNs, the SIHG-4 achieves a relatively lower performance compared to SIHG-3.

5.4 Embedding Visualization (RQ4)

To evaluate the importance of high-order topology and hierarchy preservation, we conduct experiments on the test set of the Bitcoin-Alpha dataset, and visualize the node-pair embeddings with PCA in Figure 4. The features of the compared baselines, *i.e.*, SGCN, SiGAT, SNEA are extracted before passing them to the classifier. The embeddings are scattered as circles in the projected 3D subspace, with different colors indicating the edge polarities *i.e.*, red represents friendship and blue represents antagonism. In contrast to existing graph models, the proposed SIHG are more powerful to preserve tree structure, where nodes close to the center are generally higher in the hierarchy of the tree.

5.5 Interpretability for Social Theories (RQ5)

In order to study the interpretability of two fundamental social theories, we run experiments on the Bitcoin-Alpha

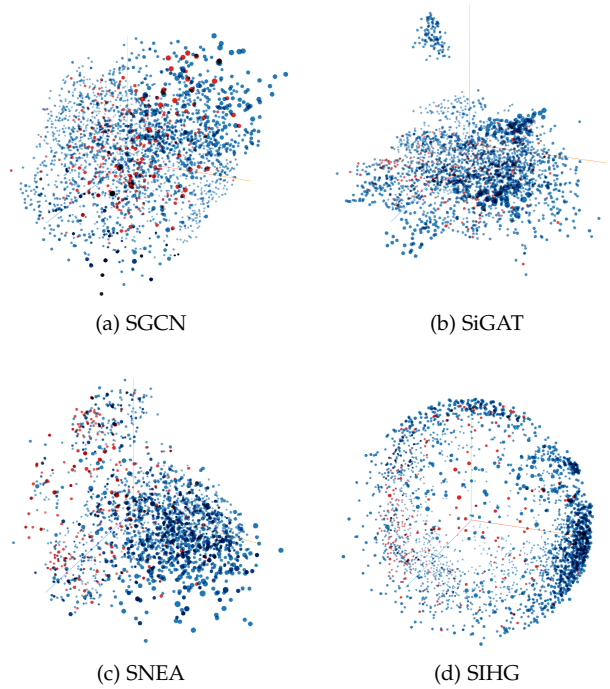


Fig. 4: The visualization of the learned embeddings by graph-based baselines and the proposed SIHG with Hyperboloid model on the Bitcoin-Alpha dataset.

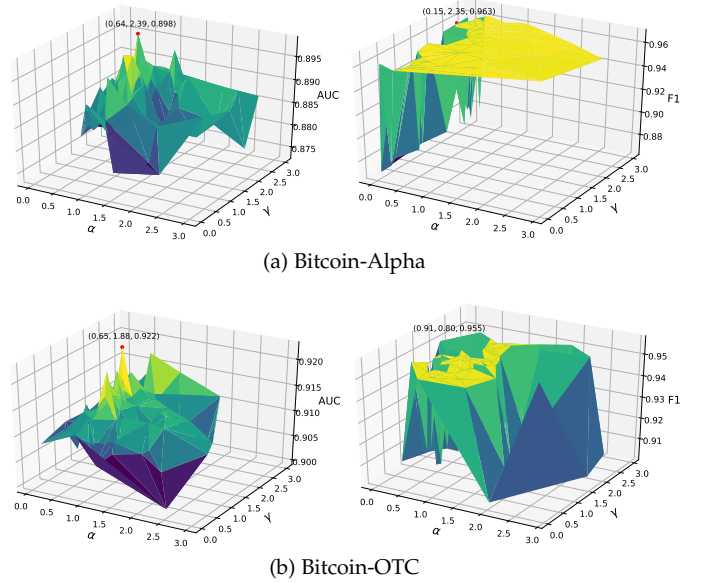


Fig. 5: The impact of loss coefficients α and γ on signed link prediction. The best trial is marked with a red point.

dataset. We extract the signed attention maps of $w_{ik}^{-(l)}$ and $w_{ij}^{-(l)}$ in the positive and negative aggregation branches at the second graph layer ($l = 2$), respectively. The attention maps are plotted in Figure 6 with D3.js. Recalling the aggregation paths in Figure 2, we can clearly discriminate the social rules by comparing the sign of attention score for each edge. For instance, the negative edge attention score in $w_{ij}^{-(2)}$ stands for structural balance theory, and the positive

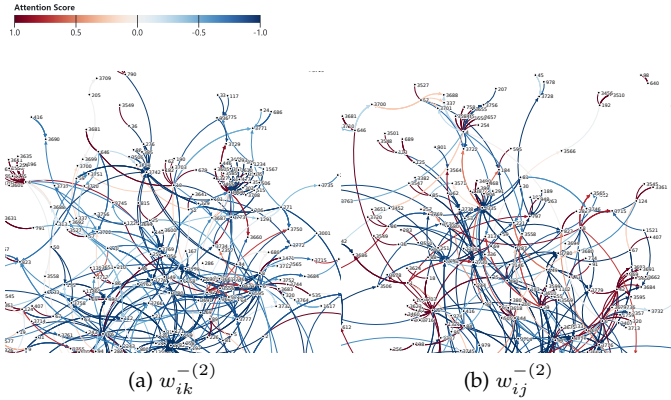


Fig. 6: The visualization of the signed attention map extracted from the proposed SIHG. Best viewed in color.

one for status theory. The signed attention learned is crucial to provide interpretation of the sociological mechanisms behind the given signed networks.

6 RELATED WORK

6.1 Signed Network Embedding

Different from unsigned networks [8]–[14] that only consist of positive links, signed networks further consider negative links with more valuable information [20]. The root of modeling signed networks lies in two important sociological theories [19], *i.e.*, balance theory and status theory. Motivated by social balance theory, Chiang *et al.* [36] extended weighted kernel k-means clustering to the signed network setting, by considering a signed variant of Laplacian matrix, which can be used as the basis for graph kernels. Similarly, Zheng *et al.* [30] applied random walk normalized to analyze signed graphs, which can be embedded in a lower-dimensional space that reveals the global similarity between nodes. Hsieh *et al.* [37] reformulated the sign inference problem as a low-rank matrix completion problem and proved that the missing links can be recovered under certain conditions.

Different from the above-mentioned works that learn node representations by spectral analysis or matrix factorization, another line of work jointly aggregates and propagates information in neural networks. SNE [38] optimizes a Skip-Gram like objective function by the maximum likelihood estimation and incorporates two signed vectors to represent the positive or negative edges with a log-bilinear model. Guided by the extended balance theory, SiNE [31] introduces a new objective function for signed network embedding, adding virtue nodes to enhance the training process. To improve algorithmic efficiency, SIDE [32] is built upon a truncated random walk, which aims to represent proximity in signed directed networks as a compact low-dimensional vector. To maintain structural balance in higher-order neighborhoods, SIGNet [33] leverages a new targeted node sampling strategy for random walks in directed signed networks. Of late, SGCN [15] is proposed, which generalizes GCN [39] to signed networks and applies a mean pooling strategy to aggregate messages from neighboring nodes according to balance theory. With the advent

in the self-attention mechanism, SiGAT [21] utilizes the graph attention networks (GAT) to embed different motifs in directed signed networks. Similarly, SNEA [16] proposes a graph attention layer and provides a more universal way to aggregate information through both positive and negative links based on balance theory. Nonetheless, the existing approaches biasedly rely on the balance and/or status theory for edge sign prediction, which may be easily violated in practice. In our proposed SIHG framework, the principle of mutual information maximization guides the model to infer edge polarities from the informative positive and negative node neighbors, where the aggregation paths are learned by the signed attention module and two social theories are thus naturally unified.

6.2 Mutual Information Estimation

Mutual Information (MI) estimation, quantifying the amount of shared information between a pair of random variables, has been playing a pivotal role in representation learning [24] and wide applications [40]. MI maximization can be used to extract representations that are highly relevant to the target task, or controlling the amount of information between the learned representations and the original data [41]–[43]. While effective, few of the prior mutual information estimators can generalize to deep neural networks due to the high dimensionality and sample size. In order to overcome the intractability of MI in the presence of high-dimensional and continuous data, Mutual Information Neural Estimation (MINE) [25] makes the estimation of MI on deep neural networks feasible via training a statistics network to distinguish samples coming from the joint distribution and the product of marginals of two random variables. Different from MINE that employs a lower-bound to the MI based on the Donsker-Varadhan representation [26] of the KL-divergence, the Jensen-Shannon MI estimator (JSD) [44] follows the formulation of f-GAN KL-divergence. Our proposed SIHG shares the same spirit with the mutual information estimators, which aims to mine the informative representations oriented by the task. But instead of using for unsupervised learning, we, *for the first time*, adapt the mutual information to guide the aggregation in the deep graph model and validate its effectiveness on a practical signed link prediction task.

7 CONCLUSION

In this work, we propose a deep SIHG framework for the signed link prediction in the presence of large-scale signed social networks. Different from the existing approaches which rely on balance or status theory, we automatically select the aggregation path and reconcile the two theories by maximizing the mutual information between the learned node embeddings and the edge polarities. Experiments evidence the effectiveness of our proposed approach over the state-of-the-art methods, especially improving the AUC scores by up to 13.0%.

ACKNOWLEDGMENTS

This work is partially supported by ARC FT130101530 and NSFC No. 61628206.

REFERENCES

- [1] R. Márquez and R. Weber, "Overlapping community detection in static and dynamic social networks," in *Proc. ACM International Conference on Web Search and Data Mining, WSDM*, 2019, pp. 822–823.
- [2] M. Sachan, A. Dubey, S. Srivastava, E. P. Xing, and E. H. Hovy, "Spatial compactness meets topical consistency: Jointly modeling links and content for community detection," in *Proc. ACM International Conference on Web Search and Data Mining, WSDM*, 2014, pp. 503–512.
- [3] S. P. Bhatt, S. Padhee, A. P. Sheth, K. Chen, V. L. Shalin, D. Doran, and B. S. Minnery, "Knowledge graph enhanced community detection and characterization," in *Proc. ACM International Conference on Web Search and Data Mining, WSDM*, 2019, pp. 51–59.
- [4] Z. Jiang, H. Liu, B. Fu, Z. Wu, and T. Zhang, "Recommendation in heterogeneous information networks based on generalized random walk model and bayesian personalized ranking," in *Proc. ACM International Conference on Web Search and Data Mining, WSDM*, 2018, pp. 288–296.
- [5] P. P. Analytis, D. Barkoczi, P. Lorenz-Spreen, and S. Herzog, "The structure of social influence in recommender networks," in *Proc. International Conference on World Wide Web, WWW*, 2020, pp. 2655–2661.
- [6] A. Breuer, R. Eilat, and U. Weinsberg, "Friend or faux: Graph-based early detection of fake accounts on social networks," in *WWW '20: The Web Conference 2020, Taipei, Taiwan, April 20-24, 2020*, 2020, pp. 1287–1297. [Online]. Available: <https://doi.org/10.1145/3366423.3380204>
- [7] B. C. Molokwu, "Event prediction in complex social graphs using one-dimensional convolutional neural network," in *Proc. International Joint Conference on Artificial Intelligence, IJCAI*, 2019, pp. 6450–6451.
- [8] H. Gao, J. Pei, and H. Huang, "Progan: Network embedding via proximity generative adversarial network," in *Proc. ACM SIGKDD International Conference on Knowledge Discovery & Data Mining, KDD*, 2019, pp. 1308–1316.
- [9] L. Gong, L. Lin, W. Song, and H. Wang, "JNET: learning user representations via joint network embedding and topic embedding," in *Proc. ACM International Conference on Web Search and Data Mining, WSDM*, 2020, pp. 205–213.
- [10] W. Lin, F. He, F. Zhang, X. Cheng, and H. Cai, "Initialization for network embedding: A graph partition approach," in *Proc. ACM International Conference on Web Search and Data Mining, WSDM*, 2020, pp. 367–374.
- [11] X. Huang, Q. Song, J. Li, and X. Hu, "Exploring expert cognition for attributed network embedding," in *Proc. ACM International Conference on Web Search and Data Mining, WSDM*, 2018, pp. 270–278.
- [12] Y. Ma, Z. Ren, Z. Jiang, J. Tang, and D. Yin, "Multi-dimensional network embedding with hierarchical structure," in *Proc. ACM International Conference on Web Search and Data Mining, WSDM*, 2018, pp. 387–395.
- [13] J. Qiu, Y. Dong, H. Ma, J. Li, K. Wang, and J. Tang, "Network embedding as matrix factorization: Unifying deepwalk, line, pte, and node2vec," in *Proc. ACM International Conference on Web Search and Data Mining, WSDM*, 2018, pp. 459–467.
- [14] H. Wang, F. Zhang, M. Hou, X. Xie, M. Guo, and Q. Liu, "SHINE: signed heterogeneous information network embedding for sentiment link prediction," in *Proc. ACM International Conference on Web Search and Data Mining, WSDM*, 2018, pp. 592–600.
- [15] T. Derr, Y. Ma, and J. Tang, "Signed graph convolutional networks," in *Proc. IEEE International Conference on Data Mining, ICDM*, 2018, pp. 929–934.
- [16] Y. Li, Y. Tian, J. Zhang, and Y. Chang, "Learning signed network embedding via graph attention," in *Proc. Conference on Artificial Intelligence, AAAI*, 2020, pp. 4772–4779.
- [17] D. Cartwright and F. Harary, "Structural balance: a generalization of heider's theory," *Psychological review*, vol. 63, no. 5, p. 277, 1956.
- [18] R. V. Guha, R. Kumar, P. Raghavan, and A. Tomkins, "Propagation of trust and distrust," in *Proc. International Conference on World Wide Web, WWW*, 2004, pp. 403–412.
- [19] J. Leskovec, D. P. Huttenlocher, and J. M. Kleinberg, "Signed networks in social media," in *Proc. International Conference on Human Factors in Computing Systems, CHI*, 2010, pp. 1361–1370.
- [20] —, "Predicting positive and negative links in online social networks," in *Proc. International Conference on World Wide Web, WWW*, 2010, pp. 641–650.
- [21] J. Huang, H. Shen, L. Hou, and X. Cheng, "Signed graph attention networks," in *Proc. International Conference on Artificial Neural Networks, ICANN*, 2019, pp. 566–577.
- [22] I. Chami, Z. Ying, C. Ré, and J. Leskovec, "Hyperbolic graph convolutional neural networks," in *Proc. Advances in Neural Information Processing Systems, NeurIPS*, 2019, pp. 4869–4880.
- [23] Q. Liu, M. Nickel, and D. Kiela, "Hyperbolic graph neural networks," in *Proc. Advances in Neural Information Processing Systems, NeurIPS*, 2019, pp. 8228–8239.
- [24] R. Linsker, "Self-organization in a perceptual network," *IEEE Computer*, vol. 21, no. 3, pp. 105–117, 1988.
- [25] M. I. Belghazi, A. Baratin, S. Rajeswar, S. Ozair, Y. Bengio, R. D. Hjelm, and A. C. Courville, "Mutual information neural estimation," in *Proc. International Conference on Machine Learning, ICML*, 2018, pp. 530–539.
- [26] M. D. Donsker and S. R. S. Varadhan, "Asymptotic evaluation of certain markov process expectations for large time. iv," *Communications on Pure and Applied Mathematics*, vol. 36, no. 2, pp. 183–212, 1983.
- [27] S. Kumar, F. Spezzano, V. S. Subrahmanian, and C. Faloutsos, "Edge weight prediction in weighted signed networks," in *Proc. IEEE International Conference on Data Mining, ICDM*, 2016, pp. 221–230.
- [28] S. Kumar, B. Hooi, D. Makhija, M. Kumar, C. Faloutsos, and V. S. Subrahmanian, "REV2: fraudulent user prediction in rating platforms," in *Proc. ACM International Conference on Web Search and Data Mining, WSDM*, 2018, pp. 333–341.
- [29] C. Eckart and G. Young, "The approximation of one matrix by another of lower rank," *Psychometrika*, vol. 1, no. 3, pp. 211–218, 1936.
- [30] Q. Zheng and D. B. Skillicorn, "Spectral embedding of signed networks," in *Proc. SIAM International Conference on Data Mining, SDM*, 2015, pp. 55–63.
- [31] M. R. Islam, B. A. Prakash, and N. Ramakrishnan, "Signet: Scalable embeddings for signed networks," in *Proc. Advances in Knowledge Discovery and Data Mining - Pacific-Asia Conference, PAKDD*, 2018, pp. 157–169.
- [32] J. Kim, H. Park, J. Lee, and U. Kang, "SIDE: representation learning in signed directed networks," in *Proc. International Conference on World Wide Web, WWW*, 2018, pp. 509–518.
- [33] M. R. Islam, B. A. Prakash, and N. Ramakrishnan, "Signet: Scalable embeddings for signed networks," in *Proc. Advances in Knowledge Discovery and Data Mining - Pacific-Asia Conference, PAKDD*, 2018, pp. 157–169.
- [34] A. Paszke, S. Gross, F. Massa, A. Lerer, J. Bradbury, G. Chanan, T. Killeen, Z. Lin, N. Gimelshein, L. Antiga, A. Desmaison, A. Köpf, E. Yang, Z. DeVito, M. Raison, A. Tejani, S. Chilamkurthy, B. Steiner, L. Fang, J. Bai, and S. Chintala, "Pytorch: An imperative style, high-performance deep learning library," in *Proc. Advances in Neural Information Processing Systems, NeurIPS*, 2019, pp. 8024–8035.
- [35] T. Akiba, S. Sano, T. Yanase, T. Ohta, and M. Koyama, "Optuna: A next-generation hyperparameter optimization framework," in *Proc. ACM SIGKDD International Conference on Knowledge Discovery & Data Mining, KDD*, 2019, pp. 2623–2631.
- [36] K. Chiang, J. J. Whang, and I. S. Dhillon, "Scalable clustering of signed networks using balance normalized cut," in *Proc. ACM International Conference on Information and Knowledge Management, CIKM*, 2012, pp. 615–624.
- [37] C. Hsieh, K. Chiang, and I. S. Dhillon, "Low rank modeling of signed networks," in *Proc. ACM SIGKDD International Conference on Knowledge Discovery & Data Mining, KDD*, 2012, pp. 507–515.
- [38] S. Yuan, X. Wu, and Y. Xiang, "SNE: signed network embedding," in *Proc. Advances in Knowledge Discovery and Data Mining - Pacific-Asia Conference, PAKDD*, 2017, pp. 183–195.
- [39] T. N. Kipf and M. Welling, "Semi-supervised classification with graph convolutional networks," in *Proc. International Conference on Learning Representations, ICLR*, 2017.
- [40] Y. Liu, Y. Yeh, T. Fu, S. Wang, W. Chiu, and Y. F. Wang, "Detach and adapt: Learning cross-domain disentangled deep representation," in *Proc. IEEE Conference on Computer Vision and Pattern Recognition, CVPR*, 2018, pp. 8867–8876.
- [41] A. A. Alemi, I. Fischer, J. V. Dillon, and K. Murphy, "Deep variational information bottleneck," in *Proc. International Conference on Learning Representations, ICLR*, 2017.
- [42] N. Tishby, F. C. N. Pereira, and W. Bialek, "The information bottleneck method," *CoRR*, vol. physics/0004057, 2000.

- [43] A. A. Alemi, I. Fischer, and J. V. Dillon, "Uncertainty in the variational information bottleneck," *CoRR*, vol. abs/1807.00906, 2018.
- [44] R. D. Hjelm, A. Fedorov, S. Lavoie-Marchildon, K. Grewal, P. Bachman, A. Trischler, and Y. Bengio, "Learning deep representations by mutual information estimation and maximization," in *Proc. International Conference on Learning Representations, ICLR*, 2019.